[13] P. C. Sofotasios and S. Freear, "The α-κ-μ/gamma distribution: A generalized nonlinear multipath/shadowing fading model," in *Proc. Annu. IEEE India Conf.*, Hyderabad, India, 2011, pp. 1–6.
[14] N. D. Chatzidiamantis and G. K. Karagiannidis, "On the distribution of the sum of Gamma-Gamma variates and applications in RF and optical wireless communications," *IEEE Trans. Commun.*, vol. 59, no. 5, pp. 1298–1308, May 2011.
[15] P. C. Sofotasios and S. Freear, "The κ-μ extreme/Gamma distribution: A physical composite fading model," in *Proc. IEEE Wireless Commun. Netw. Conf.*, Cancun, Mexico, 2011, pp. 1398–1401.
[16] J. Y. Zhang, M. Matthaiou, Z. H. Tan, and H. B. Wang, "Performance analysis of digital communication systems over composite η-μ/Gamma fading channels," *IEEE Trans. Veh. Technol.*, vol. 61, no. 7, pp. 3114–3124, Sep. 2012.
[17] S. P. Piretti, P. C. B. Bretas, Jr., and U. S. Dias, "On the α-μ/Gamma composite distribution: Field trials and validation," in *Proc. 31st. Symp. Brasileiro de Telecomun.*, Fortaleza, Brazil, 2013, pp. 1–4.
[18] P. C. Sofotasios *et al.*, "The kappa-mu/IG composite statistical distribution in RF and FSO wireless channels," in *Proc. IEEE 78th. Veh. Technol. Conf.*, Las Vegas, NV, USA, 2013, pp. 1–5.
[19] J. F. Paris, "Statistical characterization of κ-μ shadowed fading," *IEEE Trans. Veh. Technol.*, vol. 63, no. 2, pp. 518–526, Feb. 2014.
[20] A. Abdi and M. Kaveh, "On the utility of gamma PDF in modeling shadow fading (slow fading)," in *Proc. IEEE 49th. Veh. Technol. Conf.*, Houston, TX, USA, 1999, vol. 3, pp. 2308–2312.
[21] M. D. Yacoub, "The α-μ distribution: A physical fading model for the Stacy distribution," *IEEE Trans. Veh. Technol.*, vol. 56, no. 1, pp. 27–34, Jan. 2007.
[22] U. S. Dias and M. D. Yacoub, "On the α-μ autocorrelation and power spectrum functions: Field trials and validation," in *Proc. IEEE Global Commun. Conf.*, Honolulu, HI, USA, 2009, pp. 1–6.
[23] Q. Wu, D. W. Matolak, and I. Sen, "5-GHz-band vehicle-to-vehicle channels: Models for multiple values of channel bandwidth," *IEEE Trans. Veh. Technol.*, vol. 59, no. 5, pp. 2620–2625, Jun. 2010.
[24] P. Karadimas, E. D. Vagenas, and S. A. Kotsopoulos, "On the Scatterers' mobility and second order statistics of narrowband fixed outdoor wireless channels," *IEEE Trans. Wireless Commun.*, vol. 9, no. 7, pp. 2119–2124, Jun. 2010.
[25] P. K. Chong, S.-E. Yoo, S. H. Kim, and D. Kim, "Wind-blown foliage and human-induced fading in ground-surface narrowband communications at 400 MHz," *IEEE Trans. Veh. Technol.*, vol. 60, no. 4, pp. 1326–1336, May 2011.
[26] A. Michalopoulou *et al.*, "Statistical analysis for on-body spatial diversity communications at 2.45 GHz," *IEEE Trans. Antennas Propag.*, vol. 60, no. 8, pp. 4014–4019, Aug. 2012.
[27] A. Michalopoulou *et al.*, "The influence of the wearable antenna type on theon-body channel modeling at 2.45 GHz," in *Proc. 7th. Eur. Conf. Antennas Propag.*, Gothenburg, Sweden, 2013, pp. 3044–3047.
[28] J. Reig and L. Rubio, "Estimation of the composite fast fading and shadowing distribution using the log-moments in wireless communications," *IEEE Trans. Wireless Commun.*, vol. 12, no. 8, pp. 3672–3681, Aug. 2013.
[29] M. Abramowitz and I. A. Stegun, *Handbook of Mathematical Functions*, 10th ed. Washington, DC, USA: NBS, 1972.
[30] A. P. Prudnikov, Y. A. Brychkov, and O. I. Marichev, *Integrals and Series: Elementary Functions*, 4th ed., vol. 1. London, U.K.: Taylor & Francis, 1998.
[31] I. S. Gradshteyn and I. M. Ryzhik, *Table of Integrals, Series, Products*, 5th ed. Burlington, MA, USA: Academic, 1994.
[32] D. J. Lewinski, "Nonstationary probabilistic target and clutter scattering models," *IEEE Trans. Antennas Propag.*, vol. 31, no. 3, pp. 490–498, May 1983.
[33] M. Nakagami, "The m-distribution—A general formula of intensity distribution of rapid fading," in *Proc. Symp. Statist. Methods Radio Wave Propag.*, New York, NY, USA, 1960, pp. 3–36.
[34] V. Erceg, S. J. Fortune, J. Ling, A. J. Rustako, Jr., and R. A. Valenzuela, "Comparisons of a computer-based propagation prediction tool with experimental data collected in urban microcellular environments," *IEEE J. Select. Areas Commun.*, vol. 15, no. 4, pp. 677–684, May 1997.
[35] A. P. Prudnikov, Y. A. Brychkov, and O. I. Marichev, *Integrals and Series: Special Functions, Additional Chapters*, vol. 3, 2nd ed. Moscow, Russia: Fizmatlit, 2003, (in Russian).
[36] A. P. Prudnikov, Y. A. Brychkov, and O. I. Marichev, *Integrals and Series: Special Functions*, vol. 2, 3rd ed. New York, NY, USA: Gordon and Breach, 1992.

On the Throughput of Hybrid-ARQ Under Statistical Queuing Constraints

Yi Li, Mustafa Cenk Gursoy, and Senem Velipasalar

***Abstract*—Hybrid automatic repeat request (HARQ) is a high-performance communication protocol, leading to the effective use of the wireless channel and the resources with only limited feedback about the channel state information (CSI) to the transmitter. In this paper, the throughput of HARQ with incremental redundancy (IR) and fixed transmission rate is studied in the presence of statistical queuing constraints imposed as limitations on buffer overflow probabilities. In particular, tools from the theory of renewal processes and stochastic network calculus are employed to characterize the maximum arrival rates that can be supported by the wireless channel when HARQ-IR is adopted. Effective capacity is employed as the throughput metric, and a closed-form expression for the effective capacity of HARQ-IR is determined for small values of the quality-of-service (QoS) exponent. The impact of the fixed transmission rate, queuing constraints, and hard-deadline limitations on the throughput is investigated, and comparisons with type-I HARQ and HARQ with Chase Combining are provided.**

***Index Terms*—Cumulant-generating function, deadline constraints, effective capacity, fading channel, hybrid automatic repeat request (ARQ) (HARQ) with incremental redundancy (IR) (HARQ-IR), queuing constraints, renewal processes.**

I. Introduction

Recent years have witnessed a significant growth in the wireless transmission of multimedia content. For instance, as noted in the Cisco Visual Networking Index [1], mobile video traffic was 53% of the mobile data traffic by the end of 2013 and is predicted to grow, quickly, which will account for 69% of the traffic by 2018. Such multimedia traffic requires certain queuing constraints, e.g., in terms of delay, buffer overflow, or packet drop/loss probabilities, so that acceptable performance levels can be guaranteed for the end users. However, satisfying the queuing requirements and providing performance guarantees are challenging in volatile wireless environments in which channel conditions vary over time randomly due to mobility and changing environment. For improved reliability and robustness in wireless transmissions as well as efficient resource allocation, one strategy is to adapt the transmissions according to the channel conditions. In particular, if channel state information (CSI) is available at the transmitter, adaptive modulation and coding (AMC) schemes can be employed, and transmission power and rate can be varied depending on the channel fading conditions [2]. The required instantaneous CSI can be fed back from the receiver or estimated by the transmitter. With full CSI at the transmitter, AMC achieves higher throughput and/or incurs smaller outage probability [3].

Automatic repeat request (ARQ) is a feedback-based mechanism that can also be used to adapt the wireless transmissions to channel

Manuscript received October 17, 2013; revised April 24, 2014; accepted June 30, 2014. Date of publication July 23, 2014; date of current version June 16, 2015. This work was supported in part by National Science Foundation CAREER Grant CNS-1206291 and the National Science Foundation Grant CNS-1302559. The review of this paper was coordinated by Prof. H. Hassanein.

The authors are with the Department of Electrical Engineering and Computer Science, Syracuse University, Syracuse, NY 13244 USA (e-mail: yli33@syr.edu; mcgursoy@syr.edu; svelipas@syr.edu).

Color versions of one or more of the figures in this paper are available online at http://ieeexplore.ieee.org.

Digital Object Identifier 10.1109/TVT.2014.2342154

conditions. Different from AMC, ARQ can work with limited CSI at the transmitter. In ARQ schemes, while successfully decoded packets are confirmed with an acknowledgment (ACK) feedback from the receiver, erroneous receptions trigger a negative ACK (NACK) from the receiver and the retransmission of the packet from the transmitter [4]. The performance of ARQ protocols has been extensively studied in the literature. In particular, delay/queuing analysis was conducted, for instance, in [5]–[7]. In [5], the mean delay experienced by a Markovian source over a wireless channel was analyzed when selective-repeat ARQ was employed. Badia *et al.* [6] investigated the packet delay statistics of the selective-repeat ARQ in Markov channels. A queuing analysis of ARQ protocols, together with AMC strategies, was presented in [7] using matrix geometric methods. In [8], the energy efficiency of fixed-rate transmissions was analyzed under statistical queuing constraints when a simple ARQ scheme was employed in outage events.

Combining pure ARQ with error control coding increases the probability of successful transmission and results in the more powerful hybrid ARQ (HARQ) protocols [9]. In particular, better adaptation to channel conditions and higher throughput can be achieved by employing HARQ with incremental redundancy (IR) (HARQ-IR). In HARQ-IR, each packet is encoded into a long code word consisting of a number of subblocks. Initially, the first subblock is transmitted to the receiver. If the packet is decoded correctly using only the first subblock of the code word, the receiver sends an ACK, and the transmitter initiates the transmission of a new packet. In the case of a decoding failure and the reception of a NACK from the receiver, the transmitter sends the next subblock of the code word, which is jointly decoded at the receiver with the previously received subblock. Therefore, at the receiver, information accumulates with the reception of each subblock until the current packet is decoded successfully. The throughput of HARQ protocols was studied in [10] from an information-theoretic perspective, and it was shown that the throughput of HARQ-IR could approach the ergodic capacity for large transmission rates with only limited CSI. More recently, the performance of HARQ in Rayleigh block-fading channels was investigated via a mutual information-based analysis in [11], and long-term average rates achieved with HARQ were characterized under constraints on the outage probability and the maximum number of HARQ rounds. In [12], the tradeoff between energy efficiency and transmission delay in wireless multiuser systems employing HARQ-IR was studied.

In this paper, different from prior work, we analyze the throughput of HARQ-IR protocols in the presence of statistical queuing requirements imposed as constraints on the buffer overflow probability. In particular, we employ the effective capacity formulation [13] to characterize the maximum constant arrival rates that can be supported by wireless systems employing HARQ-IR protocols while providing statistical queuing guarantees at the same time.

The rest of this paper is organized as follows. In Section II, we introduce the channel model and describe the HARQ-IR scheme. In Section III, we provide our main result on the effective capacity of HARQ-IR in terms of the statistical properties of random transmission time and discuss the impact of queuing requirements and hard-deadline constraints. Numerical results are given in Section IV, and the paper is concluded in Section V. The proof of the main result is relegated to the Appendix.

II. System Model

A. Fading Channel

We consider a point-to-point wireless link and assume that block fading is experienced in the channel. More specifically, in each block duration of T_s seconds, fading is assumed to stay fixed and then change independently in the subsequent block. We assume that transmissions occur in blocks, and one fading block is our basic time unit throughout this paper. In each block duration, the transmitter sends m symbols to the receiver. In the ith block, the transmitter sends the m-dimensional signal vector $\mathbf{x}_i$ with average energy $\mathbb{E}\{\|\mathbf{x}_i\|^2\} = m\mathcal{E}$, and the received discrete time signal can be expressed as

$$\mathbf{y}_i = h_i\mathbf{x}_i + \mathbf{n}_i \quad i = 1, 2, \ldots \tag{1}$$

where h_i is the channel fading coefficient in this time block and $\mathbf{n}_i$ denotes the noise vector with independent and identically distributed (i.i.d.) complex circularly symmetric Gaussian components with zero mean and variance N_0. Then, the instantaneous capacity in each fading block can be expressed as

$$C_i = T_s B \log_2(1 + \text{SNR} z_i) \quad \text{bits/block} \tag{2}$$

where B is the system bandwidth, T_s is the block duration, $\text{SNR} = (\mathbb{E}\{\|\mathbf{x}\|^2\})/(E\{\|\mathbf{n}\|^2\}) = (m\mathcal{E})/(mN_0) = \mathcal{E}/N_0$ represents the transmitted average signal-to-noise ratio, and $z_i = |h_i|^2$ denotes the magnitude square of the fading coefficient.

B. HARQ-IR With Fixed-Rate Transmissions

We assume that the transmitter sends information at the constant rate of R bits/block,[1] and a Type-II HARQ-IR protocol is employed for reliable reception. In this scheme, the messages at the transmitter are encoded according to a certain codebook, and the code words are divided into a number of subblocks of the same length. During each fading block, only one subblock is sent to the receiver. At the receiver side, the transmitted message is decoded according to the current received subblock combined with the previously received subblocks related to the current transmitted message. In this case, information accumulates at the receiver side. According to the information-theoretical results [10], the receiver can decode the transmitted message at the end of the Mth subblock without error only if R satisfies

$$R < T_s B \sum_{i=1}^{M} \log_2(1 + \text{SNR} z_i). \tag{3}$$

Hence, with the aforementioned characterization, we consider the maximum achievable rates of HARQ with an information-theoretic perspective as in [10]. Indeed, a coding strategy for HARQ-IR is described in detail in [10] for messages to be decoded successfully when (3) is satisfied. Hence, if (3) is satisfied, the receiver gets R bits of information, an ACK feedback signal is sent, and the first subblock of a new message is transmitted in the next interval. We assume that the decoder at the receiver has the ability to detect transmission errors reliably. Therefore, if R does not satisfy (3), the receiver detects the error and sends a NACK feedback to the transmitter, triggering the transmission of the next subblock of the same message in the subsequent transmission interval.

We define the random transmission time T of a message as

$$T = \min\left\{ M : R < T_s B \sum_{i=1}^{M} \log_2(1 + \text{SNR} z_i) \right\}. \tag{4}$$

[1]More accurately, we assume that the transmitter, after each successful transmission, attempts to send R bits within the next transmission duration. If the transmitted code word is successfully decoded in the first fading block, the received data rate is R bits/block. If successful decoding occurs at the end of the Mth fading block, the received data rate is R/M bits/block.

Hence, T denotes the number of block-fading channel uses needed to successfully send a message. In our HARQ-IR model, if a renewal event occurs when the receiver decodes the transmitted message correctly, therefore T describes the interarrival time (in terms of number of fading blocks) between consequent renewal events.

It is shown in [10] that the throughput of this HARQ-IR scheme is given by

$$\gamma = \frac{R}{\mathbb{E}\{T\}} = \frac{R}{\mu_1} \tag{5}$$

where μ_1 denotes the expected value of T. Additionally, it is proven in [10] that, as $R \to \infty$, the throughput approaches the ergodic capacity, i.e.,

$$\lim_{R\to\infty} \gamma = \mathbb{E}\left\{T_s B \log_2(1+\mathrm{SNR} z_i)\right\} = \mathbb{E}\{C_i\}. \tag{6}$$

III. Effective Capacity of the Hybrid Automatic Repeat Request-Incremental Redundancy Scheme

We assume that the transmitter operates under statistical queuing constraints imposed as limitations on the buffer overflow probability. More specifically, we assume that the buffer overflow probability satisfies

$$\theta = -\lim_{\tau\to\infty} \frac{\log_e \Pr(Q \geq \tau)}{\tau} \tag{7}$$

where Q is the stationary queue length, and τ is an overflow threshold. The above limiting formulation implies that, for sufficiently large threshold τ, we have

$$\Pr(Q \geq \tau) \approx e^{-\theta\tau}. \tag{8}$$

Hence, the overflow probability decays exponentially fast with the rate controlled by the quality-of-service (QoS) exponent θ. The larger the θ, the smaller the buffer overflow probability becomes. Hence, larger θ implies that stricter queuing constraints are being imposed.

Such asymptotic buffer overflow constraints allow the use of large deviation techniques and were considered, for instance, in [14] and [15] in the context of the theory of effective bandwidth, which identifies the minimum constant service rate needed to support a time-varying arrival rate while the buffer overflow probability satisfies (7). In [13], the notion of effective capacity was introduced in order to analyze the system throughput under such constraints. More specifically, effective capacity provides the maximum constant arrival rates that can be supported with time-varying wireless transmission rates while satisfying (7). Effective capacity is essentially a dual concept and can be characterized using the theory of effective bandwidth. For instance, as shown in [16], the buffer overflow probability behaves as in (7) for a given QoS exponent θ if the arrival process $a[i]$ and departure process $s[i]$ satisfy

$$\Lambda_a(\theta) = -\Lambda_s(-\theta) \tag{9}$$

where $\Lambda_r(\theta) = \lim_{t\to\infty}(1/t)\log_e \mathbb{E}\{\mathrm{e}^{\theta\sum_{i=1}^{i=t} r[i]}\}$ denotes the asymptotic logarithmic moment-generating function of the process $r[i]$. When the arrival rate is constant, i.e., $a[i] = a_c$, then we have $\Lambda_a(\theta) = \theta a_c$. Now, in this case, (9) implies that we should have

$$a_c = -\lim_{t\to\infty} \frac{1}{\theta t} \log_e \mathbb{E}\left\{\mathrm{e}^{-\theta\sum_{i=1}^{i=t} s[i]}\right\}. \tag{10}$$

Equivalently, for a given service process $s[i]$, the right-hand side of (10) describes the maximum constant arrival rate that can be supported for a given QoS exponent θ and is indeed the formula of the effective capacity.

In our setting, we express the effective capacity as

$$C_e = -\lim_{t\to\infty} \frac{1}{\theta t} \log_e \mathbb{E}\{\mathrm{e}^{-\theta S_t}\} \tag{11}$$

$$= -\lim_{t\to\infty} \frac{1}{\theta t} \log_e \mathbb{E}\{\mathrm{e}^{-\theta R N_t}\} \tag{12}$$

where $S_t = \sum_{i=1}^{i=t} s[i]$ is the time-accumulated service process representing the total number of bits sent until time t. In our system setting, if we denote the number of successful message transmissions until time t by N_t, then $S_t = RN_t$. Note that N_t is the number of renewals made by time t, and hence, $\{N_t\}$ can be regarded as the renewal counting process with i.i.d. interarrival intervals. More explicitly, we can define N_t as

$$N_t = \max\left\{k : \sum_{l=1}^{k} T_l < t\right\} \tag{13}$$

where $\{T_l\}$ is the i.i.d. sequence of durations of successful transmissions of consecutive messages. Note that T_l is the number of fading blocks needed to successfully decode the lth message. Renewals occur when the receiver decodes a packet successfully, and N_t is the number of renewal events (or, equivalently, the number of instances that R bits of information has been successfully received) up until time t.

Using the properties of renewal processes, we obtain the following closed-form expression of the effective capacity for small θ values in terms of the statistical averages of the random transmission time T.

Theorem 1: For the HARQ-IR scheme with fixed-rate transmissions, the effective capacity in (12) has the following first-order expansion with respect to the QoS exponent θ around $\theta = 0$:

$$C_e = \frac{R}{\mu_1} - \frac{R^2\sigma^2}{2\mu_1^3}\theta + o(\theta) \tag{14}$$

where R is the fixed transmission rate, μ_1 and σ^2 are the mean and variance of the random transmission time T, and θ is the QoS exponent. Note that μ_1 and σ^2 are also functions of R. Finally, $o(\theta)$ represents the terms that vanish faster than θ as $\theta \to 0$, i.e., $\lim_{\theta\to 0}(o(\theta)/\theta) = 0$.

Proof: See in the Appendix.

To calculate the effective capacity, we need the mean and variance of the transmission time. For the HARQ-IR scheme, the distribution of T is not available in closed form, and hence, we resort to Monte Carlo simulations to obtain μ_1 and σ^2.

Remark 1: We note that, if no queuing constraints are imposed and, hence, $\theta = 0$, the effective capacity expression in (14) specializes to $C_e = R/\mu_1$, and therefore, we recover the throughput formulation obtained in [10]. Additionally, we notice in (14) that, since $R \geq 0$, $\mu_1 \geq 0$, and $\sigma^2 \geq 0$, the introduction of the queuing constraints even with small QoS exponent θ leads to a loss in the throughput, which was quantified by the term $-((R^2\sigma^2)/(2\mu_1^3))\theta$. Finally, another observation is that, while depending only on μ_1 when $\theta = 0$, the throughput starts also depending on the variance σ^2 of the random transmission time in the presence of queuing requirements. Indeed, the larger the variance, the smaller the throughput becomes in the regime of small θ.

Remark 2: By the central limit theorem for renewal counting processes [17], if the interrenewal intervals have finite variance σ^2, then we have the following convergence in distribution:

$$\frac{N_t - \frac{t}{\mu_1}}{\sigma\mu_1^{-\frac{3}{2}} t^{\frac{1}{2}}} \longrightarrow \mathcal{N}(0,1) \quad \text{as } t \to \infty.$$

Hence, the distribution of N_t tends to a Gaussian distribution with mean (t/μ_1) and variance $(\sigma^2 t/\mu_1^3)$ for large t. Now, if we approximate the distribution of N_t as

$$f_{N_t}(x) \approx \frac{1}{\sqrt{2\pi \frac{\sigma^2 t}{\mu_1^3}}} \exp\left(-\frac{\left(x - \frac{t}{\mu}\right)^2}{\frac{\sigma^2 t}{\mu_1^3}} \right) \quad \text{for large } t \tag{15}$$

then plugging the parameters into the moment-generating function of Gaussian distribution, we can obtain

$$\mathbb{E}\{\mathrm{e}^{-\theta R N_t}\} \approx \exp\left(-\frac{R}{\mu}\theta t + \frac{R^2\sigma^2}{2\mu_1^3}\theta^2 t \right) \tag{16}$$

which implies that

$$C_e = -\lim_{t\to\infty} \frac{1}{\theta t} \log_e \mathbb{E}\{\mathrm{e}^{-\theta R N_t}\} \approx \frac{R}{\mu_1} - \frac{R^2\sigma^2}{2\mu_1^3}\theta. \tag{17}$$

Remark 3: Theorem 1 can also be applied to the Type-II HARQ Chase Combining protocol. In the HARQ Chase Combining protocol, the transmitter just sends the same coded data in each retransmission, and the receiver uses maximum-ratio combining for decoding. Therefore, the packet can be decoded within M fading blocks only if R satisfies

$$R \le T_s B \log_2\left(1 + \sum_{i=1}^{M} \mathrm{SNR} z_i\right). \tag{18}$$

Since the number of successful message transmissions N_t can still be regarded as a renewal counting process and, as we show in Lemma 2 in the Appendix, all moments of the transmission time T are also finite in Chase Combining, the characterization in (14) applies to this type of HARQ as well.

Hard-Deadline Constraints: Heretofore, we have not considered any restrictions on the random transmission time T. Hence, the number of block-fading channel uses needed to successfully send a message can be arbitrarily large, particularly if the transmission rate R is also large. Indeed, as will be evidenced in the numerical results, throughput improves as R increases, but this comes at the cost of increased transmission time. On the other hand, practical systems can require hard-deadline constraints for the messages, and it is of interest to have bounds on T. For instance, we can impose

$$T \le T_u \tag{19}$$

and, hence, limit the number of HARQ rounds to send a message by T_u. More specifically, if $R > T_s B \sum_{i=1}^{T_u} \log_2(1 + \mathrm{SNR} z_i)$ and, hence, the message is not correctly decoded at the end of the T_u^{th} transmission, the message becomes outdated, and the transmitter initiates the transmission of the new message. Under this situation, the system has to operate under a queuing constraint and a deadline constraint.

We can easily see that the characterization in Theorem 1 applies in the presence of hard-deadline constraints as well once we adopt the following approach. We define $\hat{T}$ as the total duration of time that has to be taken to successfully send one message, including the periods of failed transmissions due to imposing the upper bound T_u. In this case, the count starts from 0 after a successful decoding, and transmission time $\hat{T}$ increases until the next successful decoding. Again, the renewal events happen only when the receiver can decode the packet successfully. Now, the probability that $\hat{T} = n + kT_u$, i.e., the probability that the transmission of first k messages has ended in failure due to the deadline constraint and the $(k+1)$th message is successfully transmitted after $n \le T_u$ HARQ transmissions, can be expressed as

$$\Pr\{\hat{T} = n + kT_u\} = (\Pr\{T > T_u\})^k \Pr\{T = n\} \quad \text{for } n = 1, 2, \ldots, T_u \text{ and } k = 0, 1, 2, \ldots \tag{20}$$

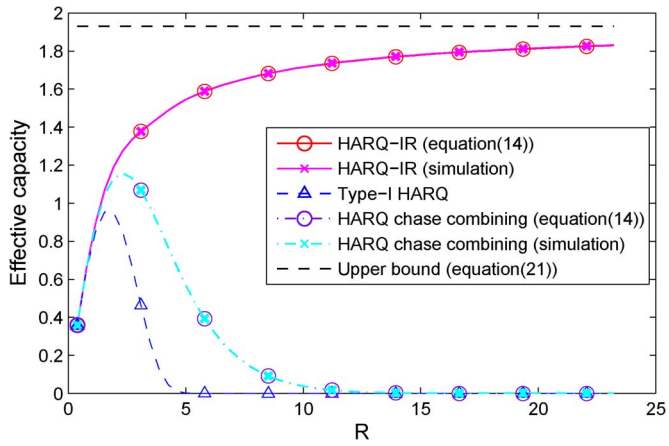

Fig. 1. Effective capacity C_e versus transmission rate R at SNR $= 6$ dB and $\theta = 0.01$ for both ARQ and HARQ-IR.

where T is as defined in (4). Under the upper bound constraint T_u, the new interrenewal time between successful message transmissions is $\hat{T}$. Hence, only the statistical description of interrenewal time changes, and the throughput formulation in (14) still applies but now with $\mu_1 = \mathbb{E}\{\hat{T}\}$ and $\sigma^2 = \mathrm{var}(\hat{T})$.

Note that the interrenewal time $\hat{T}$ can grow very fast on average with increasing rate R. This is due to the fact that the likelihood to complete the message transmission within T_u intervals becomes small for large R. Hence, many message transmissions can fail (i.e., k can become very large) before a successful transmission. More specifically, as R increases, $\Pr\{T > T_u\}$ grows, increasing the probability of large values of $\hat{T}$ and also increasing $\mu_1 = \mathbb{E}\{\hat{T}\}$. This growth is faster than what would be experienced in the absence of hard-deadline constraints, and it can lower the throughput significantly if R is larger than a threshold.

IV. Numerical Results

In this section, we provide our numerical results. In particular, we focus on the relationship between the transmission rate R and our throughput metric C_e. In our results, we both compute the first-order expansion of the effective capacity given in (14) and also simulate the HARQ-IR transmissions and estimate the effective capacity by computing $-(1/(\theta t)) \log_e \mathbb{E}\{\mathrm{e}^{-\theta R N_t}\}$ for large t. More specifically, $\mathbb{E}\{\mathrm{e}^{-\theta R N_t}\}$, the expected value, and the variance of the transmission time are determined via Monte Carlo simulations. In the numerical analysis, we assume that the fading coefficient h_i has a circularly symmetric complex Gaussian distribution with zero mean and a variance of 1. Hence, we consider a Rayleigh fading environment.

In Fig. 1, we plot the effective capacity C_e as a function of the transmission rate R for the Type-I HARQ, HARQ Chase Combining, and HARQ-IR schemes. The throughput curves of HARQ-IR and HARQ Chase Combining are plotted both by computing the first-order expansion in (14) and also via simulation. We immediately notice that, for both HARQ-IR and HARQ Chase Combining, the effective capacity approximation provided by the first-order expansion is very close to that obtained by simulation for $\theta = 0.01$. Hence, as predicted in Section III, the first-order expansion gives an accurate characterization of the throughput of HARQ-IR and HARQ Chase Combining. In the figure, we further observe that HARQ-IR significantly outperforms Type-I HARQ and HARQ Chase Combining. The throughput of Type-I HARQ initially increases and reaches its peak value at an optimal value R^* beyond which it starts to diminish. Hence, in Type-I HARQ, rates higher than the optimal R^* are leading to a large number of retransmissions and resulting in lower throughput. A similar

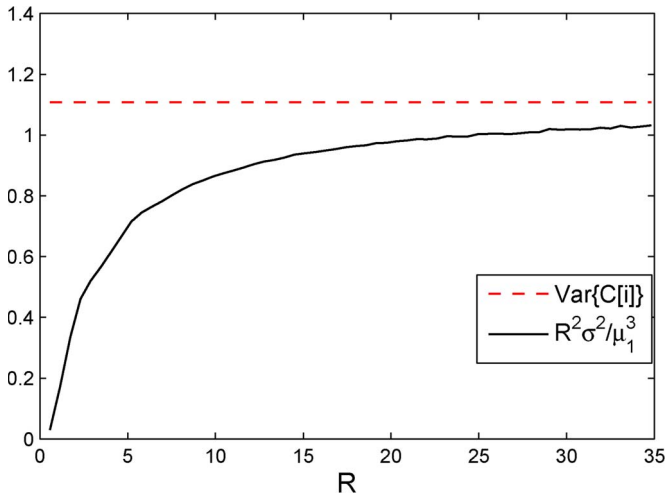

Fig. 2. $\mathrm{var}(\log_2(1+\mathrm{SNR}z))$ and $(R^2\sigma^2)/\mu_1^3$ versus transmission rate R. SNR $=6$ dB, and $\theta = 0.01$.

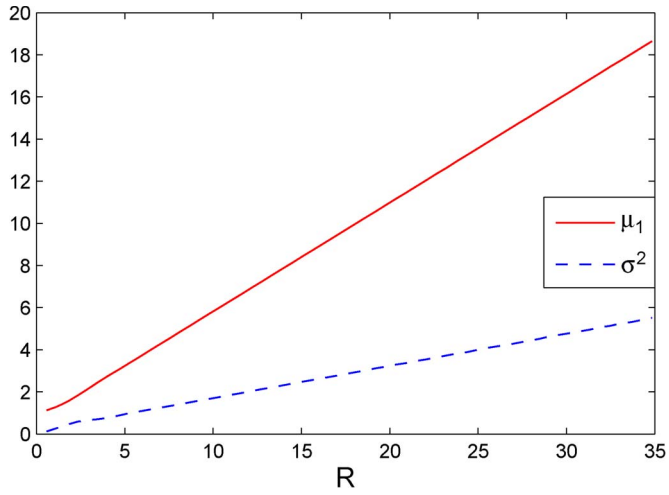

Fig. 3. Mean μ_1 and the variance σ^2 of the transmission time T versus transmission rate R. SNR $=6$ dB, and $\theta = 0.01$.

behavior is shown by HARQ Chase Combining. On the other hand, the throughput of HARQ-IR interestingly improves with increasing R and approaches

$$C_{e,\text{perfect CSI}} = -\frac{1}{\theta}\log_e \mathbb{E}\{e^{-\theta C}\}$$
$$= -\frac{1}{\theta}\log_e \mathbb{E}\left\{e^{-\theta T_s B \log_2(1+\mathrm{SNR}z)}\right\} \qquad (21)$$

which is the effective capacity of a system in which the transmitter knows the channel fading coefficients perfectly and transmits the data at the time-varying rate of $B\log_2(1+\mathrm{SNR}z)$ in each block. Note that this observation can be seen as the extension of (6) to the case with queuing constraints. Furthermore, it can be easily verified that the first-order expansion of $C_{e,\text{perfect CSI}}$ is given by

$$C_{e,\text{perfect CSI}} = \mathbb{E}\{T_s B\log_2(1+\mathrm{SNR}z)\}$$
$$- \mathrm{var}\left(T_s B\log_2(1+\mathrm{SNR}z)\right)\frac{\theta}{2} + o(\theta) \qquad (22)$$

where $\mathrm{var}(T_s B\log_2(1+\mathrm{SNR}z))$ denotes the variance of $T_s B\log_2(1+\mathrm{SNR}z)$. Comparing this expansion with (14) and noting the limiting result in (6) and the observation in Fig. 1, we expect that $(R^2\sigma^2)/\mu_1^3$ approaches $\mathrm{var}(T_s B\log_2(1+\mathrm{SNR}z))$ as R increases, which is verified numerically in Fig. 2.

The improvement in the throughput of HARQ-IR with increasing R comes at the cost of increased transmission time. This is demonstrated in Fig. 3 which shows that both the mean $\mu_1 = \mathbb{E}\{T\}$ and the variance $\sigma^2 = \mathrm{var}(T)$ of the random transmission time T increase with increasing R. Two curves in Fig. 3 are obtained using simulation results. It is interesting to note that this increased transmission time in HARQ-IR does not have a detrimental impact on the throughput under queuing constraints, which is a testament to the efficient utilization of the channel and resources by HARQ-IR. Indeed, it takes more time to send the data, but proportionally, a large amount of data is sent successfully with HARQ-IR over this extended period of time. Another observation in Fig. 3 is at the other end of the line. As R diminishes, μ_1 and σ^2 approach 1 and 0, respectively. This implies from (14) that $C_e \approx R$ for very small R, explaining the linear growth of the effective capacity curve of HARQ-IR for small R values in Fig. 1.

In Fig. 4, we plot the effective capacity versus R curve for different values of the QoS exponent θ. We see that larger θ values (and hence stricter queuing constraints) expectedly lead to lower throughput.

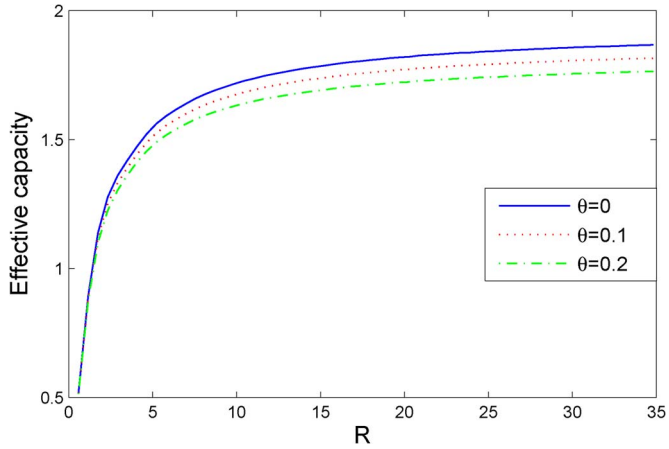

Fig. 4. Effective capacity C_e of HARQ-IR versus transmission rate R at SNR $=6$ dB for different θ values.

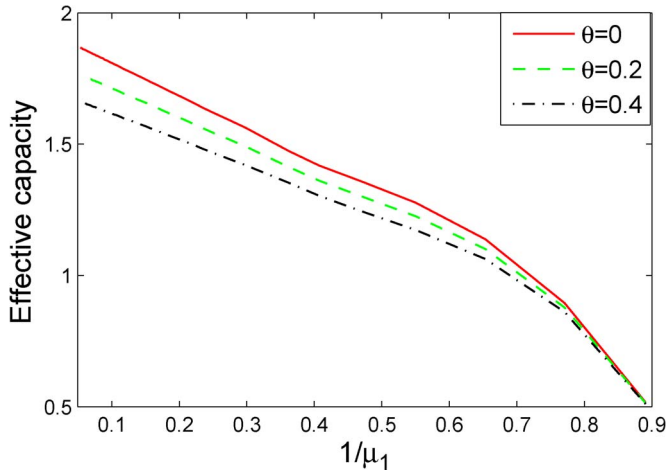

Fig. 5. Effective capacity C_e versus $(1/\mu_1)$ at SNR $=6$ dB for different θ values.

Equivalently, as θ increases, the same effective capacity is achieved by transmitting at higher rates R and, hence, by potentially experiencing larger transmission time, as depicted in Fig. 5. We note in Fig. 5 that, particularly for high effective capacities, when θ is increased, the same effective capacity is achieved at smaller values of $1/\mu_1 = 1/(\mathbb{E}\{T\})$.

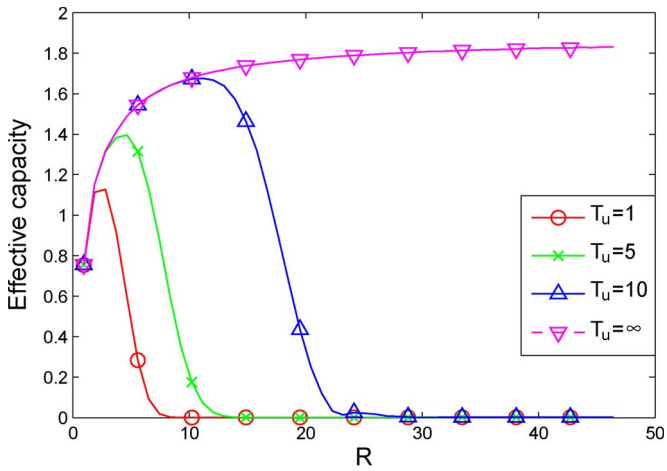

Fig. 6. Effective capacity C_e versus transmission rate R for different hard-deadline constraints. SNR $= 6$ dB, and $\theta = 0.1$.

Finally, we address the impact of hard-deadline constraints in Fig. 6. We plot C_e versus R curves for different values of the upper bound T_u on the transmission time T (or, equivalently, the number of HARQ rounds). Again, the expected value and variance of the transmission time are obtained via simulation, and effective capacities are calculated using our first-order approximation. We readily observe that, when hard-deadline constraints are imposed, there exists an optimal transmission rate $R^*(T_u)$ at which the throughput is maximized and beyond which the throughput starts diminishing. The optimal $R^*(T_u)$ and the achieved maximum throughput get larger for larger T_u while the throughput monotonically increases with increasing R when no deadline constraints are imposed, i.e., when $T_u = \infty$.

V. Conclusion

In this paper, we have investigated the throughput of HARQ-IR in the presence of queuing constraints imposed as limitations on buffer overflow probabilities. Using the statistical properties of the renewal counting process, we have identified the first-order expansion of the effective capacity of HARQ-IR in terms of the QoS exponent θ. We have shown that the loss in throughput is proportional to $((R^2\sigma^2)/(2\mu_1^3))\theta$ for small θ. We have taken into account hard-deadline constraints by imposing an upper bound on the number of HARQ rounds to send a message. We have discussed that the main result on the first-order expansion of the effective capacity holds in the presence of deadline constraints with a modified description of the transmission time. Through numerical results, we have demonstrated that increasing the transmission rate R improves the throughput monotonically in HARQ-IR and makes it approach the throughput of a system with perfect CSI at the transmitter while it initially improves and then lowers the throughput Type-I HARQ and HARQ Chase Combining. We have noted the superiority of HARQ-IR over Type-I ARQ and HARQ Chase Combining. We have also observed that increased throughput with larger R comes at the expense of longer transmission time or, equivalently, larger number of HARQ-IR rounds. We have shown that the throughput degrades when stricter queuing constraints or hard-deadline constraints are imposed. In particular, we have demonstrated that monotonic growth in the throughput with increasing R is not experienced in the presence of deadline limitations.

Appendix
Proof of Theorem 1

The proof of Theorem 1 is based on the Taylor expansion of the cumulant-generating function, which expresses C_e as a polynomial function of θ. After deriving the zeroth- and first-order coefficients of this polynomial, a closed-form expression for the first-order expansion is obtained for small θ. Before finding the polynomial approximation, we need to show that the moments of the random transmission time T are finite.

Let us denote the jth moment of the random transmission time T by

$$\mu_j = \mathbb{E}\{T^j\}. \tag{23}$$

The following characterization shows that T has finite support for any fixed transmission rate, and therefore, we have $\mu_j < \infty$ for all $1 \leq j < \infty$.

Lemma 1: If the expected value of the instantaneous capacity is strictly greater than zero, then for any fixed transmission rate R, the random transmission time T of HARQ-IR has finite support. Hence, all of its moments are finite.

Proof: Since $\{z_i\}$ is a sequence of i.i.d. random variables, by the strong law of large numbers (see [18, Sec. 7.4]), we have $(1/n)\sum_{i=1}^{n} T_s B \log_2(1+\text{SNR}z_i)$ converging to $\mathbb{E}\{T_s B \log_2(1+\text{SNR}z_i)\} = \mathbb{E}\{C_i\}$ almost surely, i.e., we have

$$\Pr\left(\lim_{n\to\infty} \frac{1}{n}\sum_{i=1}^{n} T_s B \log_2(1+\text{SNR}z_i) = \mathbb{E}\{C_i\}\right) = 1. \tag{24}$$

This almost sure convergence implies that, *with probability one*, for any given $\varepsilon > 0$, there exists a positive integer n_1 such that, for all $n \geq n_1$

$$\left|\frac{1}{n}\sum_{i=1}^{n} T_s B \log_2(1+\text{SNR}z_i) - \mathbb{E}\{C_i\}\right| \leq \varepsilon \tag{25}$$

or equivalently

$$\mathbb{E}\{C_i\} - \varepsilon \leq \frac{1}{n}\sum_{i=1}^{n} T_s B \log_2(1+\text{SNR}z_i) \leq \mathbb{E}\{C_i\} + \varepsilon. \tag{26}$$

Hence, under the assumption that $\mathbb{E}\{C_i\} > 0$, we have the following lower bound with probability one for some $0 < \varepsilon < \mathbb{E}\{C_i\}$:

$$\frac{1}{n}\sum_{i=1}^{n} T_s B \log_2(1+\text{SNR}z_i) \geq \mathbb{E}\{C_i\} - \varepsilon > 0. \tag{27}$$

Next, we consider a bound on (R/n). For a fixed transmission rate R, we have

$$\lim_{n\to\infty} \frac{R}{n} = 0. \tag{28}$$

Therefore, for any $\varepsilon_2 > 0$, there exists an integer $n_2 \geq n_1$ such that, for all $n \geq n_2$, we have

$$\frac{R}{n} \leq \varepsilon_2. \tag{29}$$

Choosing $\varepsilon_2 = E\{C_i\} - \varepsilon$ and using the bound in (27), we have, for all $n \geqslant n_2$, that

$$\frac{R}{n} \leq \frac{1}{n}\sum_{i=1}^{n} T_s B \log_2(1+\text{SNR}z_i) \tag{30}$$

or equivalently

$$R \leq \sum_{i=1}^{n} T_s B \log_2(1 + \text{SNR} z_i) \tag{31}$$

with probability one for all $n \geq n_2$. According to the condition of successful decoding in (4), (30) implies that the random transmission time T for reliably sending R bits is upper bounded by n_2 with probability one, i.e., $\Pr(T \leq n_2) = 1$.

Hence, for any given fixed transmission rate R, T has finite support as claimed in the lemma. Hence, the moments $\mu_j = \mathbb{E}\{T^j\} \leq n_2^j < \infty$ are finite for all $1 \leq j < \infty$. □

For HARQ Chase Combining, we can also show that all the moments of T are finite by applying a similar approach.

Lemma 2: If the expected value of z_i is strictly greater than zero, then for any fixed transmission rate R, the random transmission time T of HARQ Chase Combining has finite support. Hence, all of its moments are finite.

Proof: By the strong law of large numbers (see [18, Sec. 7.4]), we have $(1/n)\sum_{i=1}^{n} z_i$ converging to $\mathbb{E}\{z_i\}$ almost surely, i.e., we have

$$\Pr\left(\lim_{n\to\infty} \frac{1}{n}\sum_{i=1}^{n} z_i = \mathbb{E}\{z_i\}\right) = 1. \tag{32}$$

Similar to the proof of Lemma 1, for any given $\mathbb{E}\{z_i\} > \varepsilon > 0$, there exists a positive integer n_1 such that, for all $n \geq n_1$, we can have

$$\frac{1}{n}\sum_{i=1}^{n} z_i \geq \mathbb{E}\{z_i\} - \varepsilon > 0. \tag{33}$$

For a fixed rate R, $(2^{(R/(T_s B))} - 1)/\text{SNR}$ is also a constant. Then, we have

$$\lim_{n\to\infty} \left(2^{\frac{R}{T_s B}} - 1\right) \Big/ (n \text{ SNR}) = 0. \tag{34}$$

Therefore, for any $\varepsilon_2 > 0$, there exists an integer $n_2 \geq n_1$ such that, for all $n \geq n_2$, we have

$$\left(2^{\frac{R}{T_s B}} - 1\right) \Big/ (n \text{ SNR}) \leq \varepsilon_2. \tag{35}$$

Choosing $\varepsilon_2 = E\{z_i\} - \varepsilon$ and using the bound in (33), we have, for all $n \geq n_2$, that

$$\left(2^{\frac{R}{T_s B}} - 1\right) \Big/ (n \text{ SNR}) \leq \frac{1}{n}\sum_{i=1}^{n} z_i \tag{36}$$

or equivalently

$$R \leq T_s B \log_2\left(1 + \text{SNR}\sum_{i=1}^{n} z_i\right) \tag{37}$$

with probability one for all $n \geq n_2$. Similar as in the HARQ-IR case, we have shown that, for HARQ Chase Combining, the transmission time T also has finite support, and hence, all the moments of T are finite. □

Having shown the finiteness of all moments of T, the rest of the proof is the same for both HARQ-IR and HARQ Chase Combining. We next consider the cumulant-generating function of N_t, which is the logarithm of the moment-generating function of N_t, i.e.,

$$g(z) = \log \mathbb{E}\{\mathrm{e}^{zN_t}\}. \tag{38}$$

The cumulant-generating function can also be expressed as

$$g(z) = \sum_{j=1}^{\infty} \kappa_j(t) \frac{z^j}{j!} \tag{39}$$

where $\kappa_j(t)$ is the jth order cumulant of N_t. Examining (12), we notice that the effective capacity is proportional to the cumulant-generating function of N_t, and we can write

$$\frac{1}{\theta t}\log_e \mathbb{E}\{\mathrm{e}^{-\theta R N_t}\} = \frac{1}{\theta t}\sum_{j=1}^{\infty} \kappa_j(t)\frac{(-\theta R)^j}{j!} \tag{40}$$

$$= \sum_{j=1}^{\infty} \frac{\kappa_j(t)}{t}\frac{(-1)^j R^j}{j!}\theta^{j-1}. \tag{41}$$

Applying the theory of cumulant-generating function to our problem, the effective capacity can be expressed as

$$C_e = -\lim_{t\to\infty} \frac{1}{\theta t}\log_e \mathbb{E}\{\mathrm{e}^{-\theta R N_t}\} \tag{42}$$

$$= -\lim_{t\to\infty} \sum_{j=1}^{\infty} \frac{\kappa_j(t)}{t}\frac{(-1)^j R^j}{j!}\theta^{j-1} \tag{43}$$

$$= \sum_{j=1}^{\infty} \left(\lim_{t\to\infty} \frac{\kappa_j(t)}{t}\right)\frac{(-1)^{j+1} R^j}{j!}\theta^{j-1}$$

(by moving the limit inside the summation). (44)

It has been proven in [19] that, if the moments of T are finite, then the jth cumulant of N_t can be written as

$$\kappa_j(t) = a_j t + b_j + o(1) \tag{45}$$

for some constants a_j and b_j which depend on the moments of T. From this result, we conclude that

$$\lim_{t\to\infty} \frac{\kappa_j(t)}{t} = a_j \tag{46}$$

and hence

$$C_e = \sum_{j=1}^{\infty} a_j \frac{(-1)^{j+1} R^j}{j!}\theta^{j-1}. \tag{47}$$

Furthermore, it has been shown in [19] and [20] that

$$a_1 = \frac{1}{\mu_1} \quad \text{and} \quad a_2 = \frac{\mu_2 - \mu_1^2}{\mu_1^3} = \frac{\sigma^2}{\mu_1^3} \tag{48}$$

where $\mu_1 = \mathbb{E}\{T\}$, and $\mu_2 = \mathbb{E}\{T^2\}$ are the first and second moments of T, and σ^2 is the variance of T. Plugging in these values into (47), we readily obtain

$$C_e = \frac{R}{\mu_1} - \frac{R^2\sigma^2}{2\mu_1^3}\theta + o(\theta) \tag{49}$$

where $o(\theta)$ denotes the terms which decay faster than θ, i.e., $\lim_{\theta\to 0}(o(\theta)/\theta) = 0$. Hence, the desired characterization in Theorem 1 is proved. □

REFERENCES

[1] "Cisco visual networking index: Global mobile data traffic forecast update 2013–2018." [Online]. Available: http://www.cisco.com/c/en/us/solutions/collateral/service-provider/visual-networking-index-vni/white_paper_c11-520862.html

[2] A. Goldsmith, *Wireless Communications*. Cambridge, U.K.: Cambridge Univ. Press, 2005.

[3] A. Goldsmith and S.-G. Chua, "Variable-rate variable-power MQAM for fading channels," *IEEE Trans. Commun.*, vol. 45, no. 10, pp. 1218–1230, Oct. 1997.
[4] H. Burton and D. Sullivan, "Errors and error control," *Proc. IEEE*, vol. 60, no. 11, pp. 1293–1301, Nov. 1972.
[5] J. G. Kim and M. M. Krunz, "Delay analysis of selective repeat ARQ for a Markovian source over a wireless channel," *IEEE Trans. Wireless Commun.*, vol. 49, no. 5, pp. 1968–1981, Sep. 2000.
[6] L. Badia, M. Rossi, and M. Zorzi, "SR ARQ packet delay statistics on Markov channels in the presence of variable arrival rates," *IEEE Trans. Wireless Commun.*, vol. 5, no. 7, pp. 1639–1644, Jul. 2006.
[7] L. B. Le, E. Hossain, and M. Zorzi, "Queueing analysis for GBN and SR ARQ protocols under dynamic radio link adaptation with non-zero feedback delay," *IEEE Trans. Wireless Commun.*, vol. 6, no. 9, pp. 3418–3428, Sep. 2007.
[8] D. Qiao, M. Gursoy, and S. Velipasalar, "The impact of QoS constraints on the energy efficiency of fixed-rate wireless transmissions," *IEEE Trans. Wireless Commun.*, vol. 8, no. 12, pp. 5957–5969, Dec. 2009.
[9] S. B. Wicker, *Error Control Systems for Digital Communication and Storage*, vol. 1. Englewood Cliffs, NJ, USA: Prentice-Hall, 1995.
[10] G. Caire and D. Tuninetti, "The throughput of hybrid-ARQ protocols for the Gaussian collision channel," *IEEE Trans. Inform. Theory*, vol. 47, no. 5, pp. 1971–1988, Jul. 2001.
[11] P. Wu and N. Jindal, "Performance of hybrid-ARQ in block-fading channels: A fixed outage probability analysis," *IEEE Trans. Commun.*, vol. 58, no. 4, pp. 1129–1141, Apr. 2010.
[12] J. Choi, J. Ha, and H. Jeon, "On the energy delay tradeoff of HARQ-IR in wireless multiuser systems," *IEEE Trans. Commun.*, vol. 61, no. 8, pp. 3518–3529, Aug. 2013.
[13] D. Wu and R. Negi, "Effective capacity: A wireless link model for support of quality of service," *IEEE Trans. Wireless Commun.*, vol. 2, no. 4, pp. 630–643, Jul. 2003.
[14] C.-S. Chang, "Stability, queue length, delay of deterministic and stochastic queuing networks," *IEEE Trans. Automat. Control*, vol. 39, no. 5, pp. 913–931, May 1994.
[15] C.-S. Chang, *Performance Guarantees in Communication Networks*. New York, NY, USA: Springer-Verlag, 2000.
[16] C.-S. Chang and T. Zajic, "Effective bandwidths of departure processes from queues with time varying capacities," in *Proc. IEEE INFOCOM 14th Annu. Joint Conf. IEEE Comput. Commun. Soc.*, Apr. 1995, vol. 3, pp. 1001–1009.
[17] R. Serfozo, *Basics of Applied Stochastic Processes*. New York, NY, USA: Springer-Verlag, 2009.
[18] G. Grimmett and D. Stirzaker, *Probability and Random Processes*. London, U.K.: Oxford Univ. Press, 2001.
[19] W. L. Smith, "On the cumulants of renewal processes," *Biometrika*, vol. 46, no. 1/2, pp. 1–29, Jun. 1959.
[20] W. Feller, "Fluctuation theory of recurrent events," *Trans. Amer. Math. Soc.*, vol. 67, no. 1, pp. 98–119, Sep. 1949.

Opportunistic Network Coding Scheme for Two-Way Relay Wireless Networks: A Sum-Rate Maximization Approach

Tao Li, Ke Xiong, Yunquan Dong, and Pingyi Fan, *Senior Member, IEEE*

***Abstract*—Applying network coding (NC) in the downlink of two-way relay networks can significantly increase the throughput. However, the fading nature of wireless channels usually causes great asymmetry between two downlink channels, which can degrade the performance of NC. Therefore, it is very necessary to perform an opportunistic scheme that selects between broadcast and unicast at the relay node based on channel side information. This paper focuses on the fundamental limit of the sum rate in the downlink. To solve the maximization problem of the sum rate in the downlink, we first introduce an auxiliary variable, known as *marginal capacity income* of transmit power, and then derive the corresponding power allocation in closed-form expression and present an opportunistic switching selection strategy between broadcast/unicast. Numerical results also show that our proposed scheme achieves a larger downlink sum throughput compared with other existing known schemes.**

***Index Terms*—Marginal capacity income, opportunistic network coding (ONC), opportunistic strategy, optimal power-allocation algorithm, two-way relay networks.**

I. Introduction

By compressing multiple information flows into one single flow via finite-field algebraic operation, network coding (NC) improves system performance significantly in terms of throughput [1]. It is regarded as a promising technology for next-generation wireless networks. In particular, there is great potential to employ NC in two-way relay wireless networks due to the broadcast nature [2]. A throughput gain of 100% can be achieved in the downlink of a symmetric system if NC is used [3].

However, in a fading channel scenario, the benefit generated by NC will be weaken by the asymmetry between two downlink channels, which is caused by different path loss and randomness of channel fading. In fact, the performance of relaying scheme based on NC is even worse than store-and-forward (SF) scheme if two downlink channels at the relay node are seriously asymmetric [4]. Until now, there have been many works in the literature aiming to alleviate the

Manuscript received November 28, 2013; revised May 29, 2014; accepted July 22, 2014. Date of publication July 30, 2014; date of current version June 16, 2015. This work was supported in part by the China Major State Basic Research Development Program (973 Program) under Grant 2012CB316100(2), by the National Natural Science Foundation of China under Grant 61171064 and Grant 61321061, and by the European Union Project CoNHealth under Grant 294923. The review of this paper was coordinated by Dr. C. Yuen.

T. Li and P. Fan are with Tsinghua National Laboratory for Information Science and Technology (TNList) and the Department of Electrical Engineering, Tsinghua University, Beijing 100084, China (e-mail: litao12@mails.tsinghua.edu.cn; fpy@mail.tsinghua.edu.cn).

K. Xiong is with the School of Computer and Information Technology and the State Key Laboratory of Rail Traffic Control and Safety, Beijing Jiaotong University, Beijing 100044, China (e-mail: kxiong@bjtu.edu.cn).

Y. Dong is with the School of Communications and Electronic Engineering, Qingdao Technological University, Qingdao 266520, China (e-mail: dongyunquan@qtech.edu.cn).

Color versions of one or more of the figures in this paper are available online at http://ieeexplore.ieee.org.

Digital Object Identifier 10.1109/TVT.2014.2344131